International Journal of Solids and Structures 48 (2011) 3444–3452

Contents lists available at SciVerse ScienceDirect

International Journal of Solids and Structures

journal homepage: www.elsevier.com/locate/ijsolstr

Depth-sensing indentation of a transversely isotropic elastic layer: Second-order asymptotic models for canonical indenters

I.I. Argatov

Institute of Mathematics and Physics, Aberystwyth University, Ceredigion SY23 3BZ, Wales, UK

ARTICLE INFO

Article history:
Received 2 June 2011
Received in revised form 3 August 2011
Available online 6 September 2011

Keywords:
Unilateral contact problem
Depth-sensing indentation
Spherical indenter
Conical indenter
Berkovich indenter
Vickers indenter
Asymptotic model

ABSTRACT

Simple analytical approximations to the frictionless indentation problem for a transversely isotropic layer are obtained for spherical, conical, and pyramidal indenters as well as for axisymmetric indenters of power-low profile and self-similar non-axisymmetric indenters. These approximations are asymptotically exact in the small-contact limit. The results obtained are validated in the case of an isotropic layer for spherical and conical indenters.

1. Introduction

Depth-sensing indentation tests are widely used for determining mechanical properties of small specimens and thin films (Fischer-Cripps, 2004). Indentation testing has also proved useful for identification of mechanical properties of biological materials such as articular cartilage (Jurvelin et al., 1987; Korhonen et al., 2003). However, while the majority of analytical studies analyzing depth-sensing indentation have focused on isotropic material models, articular cartilage has been represented as a transversely isotropic layered material (Garcia et al., 1998; Wu and Herzog, 2002; Wilson et al., 2005). Recently, Batra and Jiang (2008) have reviewed the current state-of-the-art in analytical approaches to contact problems for anisotropic materials. Using Stroh's formalism, they studied the plane strain indentation of an anisotropic elastic layer. An analytical solution of the contact problem for a for transversely isotropic layer indented by a hemispherically ended punch was obtained by England (1962). Recently, the stress–strain state in a transversely isotropic layer was studied in Cortes and Garcia (2005) and Klindukhov (2009). The stress fields in the hard-coating and the soft-coating isotropic thin-film/substrate systems were analyzed by Li and Chou (1997). In a series of papers, Fabrikant (2006, 2011) has developed an analytical approach to linear (with an a priori fixed contact area) contact problems for a transversely isotropic layered medium. Nevertheless, the lack of analytical closed-form solutions for the load-displacement relationships prevents using these results for routine indentation testing. In recent years, finite element models have been developed for simulations of indentations tests for transversely isotropic materials (Korhonen et al., 2002; Li et al., 2009).

As a first approximation, force–displacement data obtained in the depth-sensing indentation tests performed with a spherical indenter are analyzed by fitting them with the Hertzian model of elastic contact, which is based on the so-called assumption of infinite sample thickness (Johnson, 1985). When the sample thickness is finite with respect to the radius of the contact area, it is well known that applications of the Hertzian model lead to systematic errors due to the infinite sample thickness assumption. The case of an isotropic elastic layer of finite thickness deposited on a rigid substrate was studied for several decades (Lebedev and Ufliand, 1958; Vorovich and Ustinov, 1959; Keer, 1964; Hayes et al., 1972; Vorovich et al., 1974; Sakamoto et al., 1996; Argatov, 2001; Dimitriadis et al., 2002). When the substrate stiffness is not high enough to neglect the substrate influence, a more complicated two-layered model for the sample-substrate system should be adopted. This issue has been addressed in the literature (Doerner and Nix, 1986; Xu and Pharr, 2006; Gao et al., 1992), where different finite sample thickness models were developed in the case of isotropic sample material. Very recently (Argatov, 2010), asymptotic models were constructed for frictionless and adhesive (no-slip) indentation of an isotropic elastic layer deposited on an isotropic elastic substrate under the assumption that the contact radius, a, is small compared with the layer thickness, h.

E-mail address: iva1@aber.ac.uk

0020-7683/$ - see front matter © 2011 Elsevier Ltd. All rights reserved.
doi:10.1016/j.ijsolstr.2011.08.011

With the advent of the atomic force microscope (ATM) as a microindenter for measuring elastic properties of biological tissues such as articular cartilage (Stolz et al., 2009), there have been new issues to deal with in describing indentation such as application of conical and pyramidal indenters along with transverse anisotropy of samples. An analytical solution of the contact problem for an isotropic elastic layer indented with a conical punch was obtained by Kalaba et al. (1976). Recently, Borodich et al. (2003) and Giannakopoulos (2006) developed different analytical approaches to indentation problems for pyramidal indenters in the case of an isotropic elastic half space, though their results can be easily generalized for the case of a transversely isotropic elastic half-space. However, to the best of the author's knowledge there have been no attempts to develop a finite sample thickness model for indentation of a transversely isotropic elastic layer with a non-spherical indenter.

Another difficulty associated with analytical modeling of microindentation of thin samples is the need to have finite sample thickness models valid in a wide range of ratio a/h, where a is the radius of the contact area, h is the sample thickness. It turns out that analytical solutions of the contact problems for relatively thick and thin elastic layers differ greatly, being strongly dependent on the value of Poisson's ratio with decreasing the layer thickness. Aleksandrov (1969) obtained an asymptotic solution when Poisson's ratio, ν, of the layer material is not very close to 0.5. The case of an incompressible layer material with $\nu = 0.5$ was first studied by Matthewson (1981) and after that in Chadwick (2002), Aleksandrov (2003). For dealing with non-axisymmetric situations, Barber (1990) developed an approximate method of Jaffar (1989) and Johnson (1985) extending their axisymmetric solutions for the three-dimensional problem of elliptical contact. Recently, analytical solutions were obtained for the indentation problems of elliptical contact for compressible (Argatov, 2005) and incompressible (Hlaváček, 2008) isotropic elastic layers.

It is known that elastic contact problems can be interpreted as inverse problems of finding the contact force and contact pressures that are necessary for imposing a prescribed displacement of the indenter and, generally, the prescribed displacement field under the indenter surface. Using Green's function approach, the problem of contact pressure evaluation for a linearly elastic material can be reduced to an integral equation with respect to the contact pressure density over the contact area. At that, the contact area itself is not known a priori for a blunt indenter. In the latter case, we have to deal with the so-called unilateral contact problem, which should be formulated as a variational inequality (Duvaut and Lions, 1972). Considering the integral transform method in contact problems for layered elastic media, Chen (1971) observed that this method was slow to converge near the edge of the contact zone, and especially for relatively thin layers. In order to overcome this shortcoming of the integral transform method, Chen and Engel (1972) introduced a new approach by replacing the exact mixed contact boundary conditions by approximate boundary conditions of the second kind. The numerical solution of Chen and Engel (1972) was reduced by Stevanovic et al. (2001) to a simple root finding procedure for the unknown contact radius, but the force–displacement relationship was not considered. Thus, numerical solving the unilateral contact problems (including finite element simulations) represents a rather tedious approach for routine AFM indentation applications (Antunes et al., 2006). That is why, in reviewing the literature on modeling the indentation problem, Dimitriadis et al. (2002) observed that simple analytical finite sample thickness models should be very helpful.

In the present paper, we develop simple approximate (but asymptotically exact in the small-contact limit) analytical solutions to the indentation problem for a transversely isotropic layer and validate the obtained asymptotic models in the case of an isotropic layer indented with a spherical or a conical indenter. The analytical method applied is similar to asymptotic techniques used previously in application to isotropic spherical nanoindentation (Argatov, 2010). The new aspect of the asymptotic analysis reported herein is the use of the asymptotic method (Argatov, 2005) based on Lagrange's formula for solving algebraic equations (De Bruijn, 1958) to derive the force–displacement relationships in explicit form. Finally, based on the present analysis, the second-order asymptotic model of the substrate effect for the incremental contact stiffness in spherical indentation (Argatov, 2010) can be generalized for conical and pyramidal indenters as well as for axisymmetric indenters of power-low profile and self-similar non-axisymmetric indenters.

2. Unilateral contact problem formulation

The unilateral frictionless contact problem for a transversely isotropic elastic layer resting on a rigid support is formulated as follows:

$$p(x_1,x_2) \geqslant 0, \quad (x_1,x_2) \in \Sigma, \tag{1}$$

$$p(x_1,x_2) > 0 \Rightarrow \int\int_{\Sigma} G_3(x_1-y_1,x_2-y_2,0)p(\mathbf{y})d\mathbf{y} = w - \Phi(x_1,x_2), \tag{2}$$

$$p(x_1,x_2) = 0 \Rightarrow \int\int_{\Sigma} G_3(x_1-y_1,x_2-y_2,0)p(\mathbf{y})d\mathbf{y} \geqslant w - \Phi(x_1,x_2). \tag{3}$$

Here, $p(x_1,x_2)$ is the contact pressure density, w is the indenter's displacement, Σ is the domain where the right-hand side of Eq. (2) is positive, $\Phi(x_1,x_2)$ is a function describing the indenter's shape, $G_3(x_1,x_2,0)$ is the linear surface influence function for the elastic layered medium.

Let ω denote the contact area, which is a subdomain of Σ. Then, the unilateral contact problem (1)–(3) is usually formulated in the form of the governing integral equation

$$\int\int_{\omega} G_3(x_1-y_1,x_2-y_2,0)p(\mathbf{y})d\mathbf{y} = w - \Phi(x_1,x_2), \tag{4}$$

where it is implicitly assumed that the contact pressure is positive inside of ω and vanishes outside of ω.

From the equilibrium equation, the external contact force, P, is related to the contact pressure density $p(x_1,x_2)$ as follows:

$$P = \int\int_{\omega} p(\mathbf{y})d\mathbf{y}. \tag{5}$$

Applying the standard two-dimensional Fourier transform technique (Sneddon, 1995; Alexandrov and Pozharskii, 2001), it can be shown (Vorovich et al., 1974) that

$$G_3(y_1,y_2,0) = \vartheta\left(\frac{1}{|\mathbf{y}|} - \frac{1}{h}\mathcal{F}\left(\frac{|\mathbf{y}|}{h}\right)\right), \tag{6}$$

where h is the layer thickness, ϑ is an elastic constant, $\mathcal{F}(t)$ is a dimensionless function given by the integral

$$\mathcal{F}(t) = \int_0^{\infty} [1 - \mathcal{L}(\lambda)]J_0(\lambda t)d\lambda \tag{7}$$

with $J_0(x)$ being the Bessel function of the first kind.

The kernel function $\mathcal{L}(\lambda)$ depends on the type of elastic layered medium.

3. Kernel function for transversely isotropic layer

The constitutive relationship for a transversely isotropic material referred to the Cartesian coordinates (x_1,x_2,x_3) with the Ox_1x_2

plane coinciding with the plane of elastic symmetry can be written in the matrix form as follows (Elliott, 1948):

$$\begin{pmatrix}\sigma_{11}\\ \sigma_{22}\\ \sigma_{33}\\ \sigma_{13}\\ \sigma_{23}\\ \sigma_{12}\end{pmatrix}=\begin{bmatrix}A_{11} & A_{12} & A_{13} & 0 & 0 & 0\\ A_{12} & A_{11} & A_{13} & 0 & 0 & 0\\ A_{13} & A_{13} & A_{33} & 0 & 0 & 0\\ 0 & 0 & 0 & 2A_{44} & 0 & 0\\ 0 & 0 & 0 & 0 & 2A_{44} & 0\\ 0 & 0 & 0 & 0 & 0 & A_{11}-A_{12}\end{bmatrix}\begin{pmatrix}\varepsilon_{11}\\ \varepsilon_{22}\\ \varepsilon_{33}\\ \varepsilon_{13}\\ \varepsilon_{23}\\ \varepsilon_{12}\end{pmatrix}.$$

For a transversely isotropic material, only five independent elastic constants are needed to describe its deformational behavior. The elastic moduli A_{11}, A_{12}, A_{13}, A_{33}, and A_{44} can be expressed in terms of the engineering elastic constants as follows (Liao and Wang, 1998):

$$A_{11}=\frac{E\left(1-\frac{E}{E'}\nu'^2\right)}{(1+\nu)\left(1-\nu-\frac{2E}{E'}\nu'^2\right)},\quad A_{12}=\frac{E\left(\nu+\frac{E}{E'}\nu'^2\right)}{(1+\nu)\left(1-\nu-\frac{2E}{E'}\nu'^2\right)},$$

$$A_{13}=\frac{E\nu'}{1-\nu-\frac{2E}{E'}\nu'^2},\quad A_{33}=\frac{E'(1-\nu)}{1-\nu-\frac{2E}{E'}\nu'^2},\quad A_{44}=G'.$$

Here, E and E' are Young's moduli in the plane of transverse isotropy and in the direction normal to it, respectively, ν and ν' are Poisson's ratios characterizing the lateral strain response in the plane of transverse isotropy to a stress acting parallel or normal to it, respectively, G' is the shear modulus in planes normal to the plane of transverse isotropy. Note also that $A_{11}-A_{12}=E/(1+\nu)$.

In the case of a transversely isotropic elastic layer bonded to a rigid base, in accordance with the known solution (Fabrikant, 2006), we have

$$\vartheta=\frac{(\gamma_1+\gamma_2)A_{11}}{2\pi\left(A_{11}A_{33}-A_{13}^2\right)}, \tag{8}$$

$$\mathcal{L}(\lambda)=1+\frac{2\left[m_+\left(\gamma_1e^{-2\lambda_1}+\gamma_2e^{-2\lambda_2}\right)-\gamma_-m_-e^{-2\lambda_1-2\lambda_2}-4\gamma_1\gamma_2e^{-\lambda_1-\lambda_2}\right]}{8\gamma_1\gamma_2e^{-\lambda_1-\lambda_2}+\gamma_-m_-(1+e^{-2\lambda_1-2\lambda_2})-\gamma_+m_+(e^{-2\lambda_1}+e^{-2\lambda_2})}. \tag{9}$$

Here, γ_1 and γ_2 are the roots of the equation

$$\gamma^4A_{11}A_{44}-\gamma^2[A_{11}A_{33}-A_{13}(A_{13}+2A_{44})]+A_{33}A_{44}=0, \tag{10}$$

and the following notation has been introduced:

$$\lambda_1=\frac{\lambda}{\gamma_1},\quad \lambda_2=\frac{\lambda}{\gamma_2},\quad \gamma_+=\gamma_1+\gamma_2,\quad \gamma_-=\gamma_1-\gamma_2, \tag{11}$$

$$m_+=m_2\gamma_1+m_1\gamma_2,\quad m_-=m_2\gamma_1-m_1\gamma_2,$$

$$m_1=\frac{A_{11}\gamma_1^2-A_{44}}{A_{13}+A_{44}},\quad m_2=\frac{A_{11}\gamma_2^2-A_{44}}{A_{13}+A_{44}}.$$

In the case of a transversely isotropic elastic layer resting on a smooth rigid base, the following representation holds true (Fabrikant, 2011):

$$\mathcal{L}(\lambda)=1+\frac{2\left[\gamma_-e^{-2\lambda_1-2\lambda_2}-\gamma_1e^{-2\lambda_1}-\gamma_2e^{-2\lambda_2}\right]}{\gamma_-(1-e^{-2\lambda_1-2\lambda_2})+\gamma_+(1-e^{-2\lambda_1}-e^{-2\lambda_2})}. \tag{12}$$

Here, λ_1, λ_2 and γ_-, γ_+ are determined by formulas (11).

We underline that the contact problem for a transversely isotropic elastic layer and the contact problem for an isotropic elastic half-space differ only by the analytical representations of the kernel function $\mathcal{L}(\lambda)$.

4. Second order asymptotic model

According to Vorovich et al. (1974), there is a neighborhood of zero on which the function (7) is represented by an absolutely convergent power series

$$\mathcal{F}(t)=\sum_{m=0}^{\infty}a_mt^{2m} \tag{13}$$

with the coefficients

$$a_m=\frac{(-1)^m}{[(2m)!!]^2}\int_0^{\infty}[1-\mathcal{L}(\lambda)]\lambda^{2m}d\lambda. \tag{14}$$

Substituting (13) into (6), we obtain

$$\vartheta^{-1}\int\!\!\int_{\omega}G_3(x_1-y_1,x_2-y_2,0)p(\mathbf{y})d\mathbf{y}=\int\!\!\int_{\omega}\frac{p(\mathbf{y})d\mathbf{y}}{\sqrt{(x_1-y_1)^2+(x_2-y_2)^2}}-\frac{1}{h}\sum_{m=0}^{\infty}\frac{a_m}{h^{2m}}\times\int\!\!\int_{\omega}\left((x_1-y_1)^2+(x_2-y_2)^2\right)^mp(\mathbf{y})d\mathbf{y}. \tag{15}$$

Now, keeping only the first term of the infinite series in (15), we replace the governing integral Eq. (4) with the following approximate equation (Argatov, 1999):

$$\vartheta\int\!\!\int_{\omega}\frac{p(\mathbf{y})d\mathbf{y}}{\sqrt{(x_1-y_1)^2+(x_2-y_2)^2}}=w+\frac{a_0}{h}\vartheta P-\Phi(x_1,x_2), \tag{16}$$

where P is the contact force related to the unknown contact pressure according to Eq. (5).

We emphasize that since the right-hand side of (13) is a series in even powers of the variable t, Eq. (16) represents the second-order asymptotic approximation even though only the first correction in (15) has been taken into account.

5. Spherical indenter

For an indenter shaped as a paraboloid of revolution, we have

$$\Phi(x_1,x_2)=\frac{1}{2R}\left(x_1^2+x_2^2\right), \tag{17}$$

where R is the curvature radius of the indenter surface at its apex.

Asymptotic solutions to the contact problem (15) in the case (17) under the assumption that the radius of the contact area, a, is small compared with the layer thickness, h, were obtained in Vorovich et al. (1974) and Argatov (2001). The fourth-order asymptotic model looks as follows (Vorovich et al., 1974):

$$p(r)=\frac{2}{\pi^2\vartheta R}\sqrt{a^2-r^2}\left\{1-\varepsilon^3\frac{8a_1}{3\pi}+O(\varepsilon^5)\right\}, \tag{18}$$

$$P=\frac{4a^3}{3\pi\vartheta R}\left\{1-\varepsilon^3\frac{8a_1}{3\pi}+O(\varepsilon^5)\right\}, \tag{19}$$

$$P=\frac{4wa}{3\pi\vartheta}\left[1+\varepsilon\frac{4a_0}{3\pi}+\varepsilon^2\left(\frac{4a_0}{3\pi}\right)^2+\varepsilon^3\left\{\left(\frac{4a_0}{3\pi}\right)^3+\frac{8a_1}{15\pi}\right\}+\varepsilon^4\left\{\left(\frac{4a_0}{3\pi}\right)^4+\frac{64a_0a_1}{45\pi^2}\right\}+O(\varepsilon^5)\right]. \tag{20}$$

Here, $r=\sqrt{x_1^2+x_2^2}$ is a polar radius, a_0 and a_1 are asymptotic constants (14), $\varepsilon=a/h$ is a small parameter.

First of all, it is clearly seen from (18)–(20) that the second correction in (15), which introduces the asymptotic constant a_1, is responsible for the terms of order ε^3. This gives another evidence

that the approximate integral Eq. (16) represents the second-order asymptotic model.

Second, the two algebraic Eqs. (19) and (20) combine three variables, namely, the contact force P, the indenter's displacement w, and the radius a of the contact area ω. From (19) and (20), it follows that

$$P=\frac{4a^3}{3\pi\vartheta R}\left(1-\varepsilon^3\frac{8a_1}{3\pi}\right), \tag{21}$$

$$w=\frac{a^2}{R}\frac{1-\varepsilon^3\frac{8a_1}{3\pi}}{1+\varepsilon\frac{4a_0}{3\pi}+\varepsilon^2\left(\frac{4a_0}{3\pi}\right)^2+\varepsilon^3\left\{\left(\frac{4a_0}{3\pi}\right)^3+\frac{8a_1}{15\pi}\right\}+\varepsilon^4\left\{\left(\frac{4a_0}{3\pi}\right)^4+\frac{64a_0a_1}{45\pi^2}\right\}}. \tag{22}$$

Eqs. (21) and (22) give a parametric representation of the load-displacement curve.

Following Argatov (2005) and using the asymptotic method based on Lagrange's formula for solving algebraic equations (De Bruijn, 1958), we can exclude the variable a from the system (21) and (22) as follows:

$$P=\frac{4h^3\alpha^3}{3\pi\vartheta R}\left\{1+\alpha\frac{2a_0}{\pi}+\alpha^2\frac{14a_0^2}{3\pi^2}+\alpha^3\left\{\frac{320a_0^3}{27\pi^3}+\frac{32a_1}{15\pi}\right\}+\alpha^4\left\{\frac{286a_0^4}{9\pi^4}+\frac{64a_0a_1}{5\pi^2}\right\}+O(\alpha^5)\right\}. \tag{23}$$

Here we introduced the notation

$$\alpha=\frac{\sqrt{wR}}{h}. \tag{24}$$

The second-order asymptotic model employing only the first asymptotic constant a_0 results in the following load-displacement relationship:

$$P=\frac{4\sqrt{R}w^{3/2}}{3\pi\vartheta}\left(1+\frac{2a_0}{\pi}\frac{\sqrt{R}}{h}w^{1/2}+\frac{14a_0^2}{3\pi^2}\frac{R}{h^2}w\right). \tag{25}$$

The contact radius is given by

$$a=\sqrt{wR}\left(1+\frac{2a_0}{3\pi}\frac{\sqrt{R}}{h}w^{1/2}+\frac{10a_0^2}{9\pi^2}\frac{R}{h^2}w\right). \tag{26}$$

Note that as it was previously shown (Argatov, 2010), with appropriate choice of the asymptotic constants a_0 and a_1, Eqs. (21) and (22) as well as Eqs. (25) and (26) are valid for a two-layered elastic medium with axisymmetric anisotropy.

6. Conical indenter

For a cone (a Rockwell indenter), we have

$$\Phi(x_1,x_2)=r\tan\theta, \tag{27}$$

where $r=\sqrt{x_1^2+x_2^2}$ is a polar radius, θ is the angle between the contact surface and the site surface of the cone.

Using the analytical solution first derived by Love (1939), we obtain a closed-form solution to Eq. (16) in the case (27) as follows:

$$p(r)=p_0\ln\left(\frac{a}{r}+\sqrt{\frac{a^2}{r^2}-1}\right). \tag{28}$$

Here, $p_0=P/(\pi a^2)$ is the mean contact pressure.

At that, the main contact parameters are connected through the system

$$w+\frac{a_0}{h}\vartheta P=\frac{\pi}{2}a\tan\theta, \tag{29}$$

$$P=\frac{a^2}{2\vartheta}\tan\theta. \tag{30}$$

Applying the asymptotic method, we can exclude the contact radius a from the system (29) and (30), arriving at the following load-displacement relationship:

$$P=\frac{2\cot\theta}{\pi^2\vartheta}w^2\left(1+\frac{4a_0}{\pi^2}\frac{w}{h}+\frac{20a_0^2}{\pi^4}\frac{w^2}{h^2}\right). \tag{31}$$

The contact radius is given by

$$a=\frac{2\cot\theta}{\pi\vartheta}w\left(1+\frac{2a_0\cot\theta}{\pi^2}\frac{w}{h}+\frac{8a_0^2\cot^2\theta}{\pi^4}\frac{w^2}{h^2}\right). \tag{32}$$

Note that we keep only three terms in the asymptotic expansions (31) and (32) according to the asymptotic accuracy of Eqs. (29) and (30).

7. Indenter of power-law profile

Let now the indenter's shape function is

$$\Phi(x_1,x_2)=Ar^\lambda, \tag{33}$$

where λ is not necessarily an even positive number.

Using the analytical solution first obtained by Galin (2008), we get a closed-form solution to Eq. (16) in the case (33) as follows:

$$p(r)=\frac{(\lambda+1)}{2}p_0\int_0^{\sqrt{1-\rho^2}}(\rho^2+\sigma^2)^{(\lambda-2)/2}d\sigma. \tag{34}$$

Here, $p_0=P/(\pi a^2)$ is the mean contact pressure, $\rho=r/a$ is the dimensionless polar radius.

The contact force P, the indenter displacement w, and the contact radius a are connected through the system

$$w+\frac{a_0}{h}\vartheta P=AN_1(\lambda)a^\lambda, \tag{35}$$

$$\vartheta P=AN_2(\lambda)a^{\lambda+1}. \tag{36}$$

Here we introduced the notation

$$N_1(\lambda)=2^{\lambda-2}\lambda\frac{\Gamma\left(\frac{\lambda}{2}\right)^2}{\Gamma(\lambda)},\quad N_2(\lambda)=\frac{2^{\lambda-1}\lambda^2}{\pi(\lambda+1)}\frac{\Gamma\left(\frac{\lambda}{2}\right)^2}{\Gamma(\lambda)} \tag{37}$$

with $\Gamma(x)$ being the gamma function.

Applying the asymptotic method, we can exclude the contact radius a from the system (35) and (36), deriving the following load-displacement relationship:

$$P=\frac{N_3(\lambda)}{\vartheta A^{1/\lambda}}w^{\frac{\lambda+1}{\lambda}}\left(1+\frac{(\lambda+1)}{\lambda}\frac{a_0}{h}\frac{N_3(\lambda)}{A^{1/\lambda}}w^{1/\lambda}+\frac{(\lambda+1)(2\lambda+3)}{2\lambda^2}\left(\frac{a_0}{h}\frac{N_3(\lambda)}{A^{1/\lambda}}\right)^2w^{2/\lambda}\right). \tag{38}$$

Here we introduced the notation

$$N_3(\lambda)=\frac{N_2(\lambda)}{N_1(\lambda)^{\frac{\lambda+1}{\lambda}}}.$$

The contact radius is given by the formula

$$a=\frac{w^{1/\lambda}}{A^{1/\lambda}N_1(\lambda)^{1/\lambda}}\left(1+\frac{1}{\lambda}\frac{a_0}{h}\frac{N_3(\lambda)}{A^{1/\lambda}}w^{1/\lambda}+\frac{(\lambda+3)}{2\lambda^2}\left(\frac{a_0}{h}\frac{N_3(\lambda)}{A^{1/\lambda}}\right)^2w^{2/\lambda}\right). \tag{39}$$

It can be checked that Eqs. (38), (39) reduce to Eqs. (25), (26) and Eqs. (31), (32) for $\lambda=2$ and $\lambda=1$, respectively.

8. Pyramidal indenters

For a pyramidal indenter, we have

$$\Phi(x_1,x_2)=\frac{r\cos\psi}{\tan\Theta},\quad 0\leqslant\psi\leqslant\Psi, \tag{40}$$

where $r=\sqrt{x_1^2+x_2^2}$ is a polar radius, ψ is a polar angle, Ψ is the angle of the periodic sector (e.g., $\pi/4$ for the Vickers indenter and $\pi/3$ for the Berkovich indenter), Θ is the angle of the pyramidal plane with its vertical axis.

Following Giannakopoulos (2006), we assume that the contact pressure for the pyramidal indenters follows a similar to (28) logarithmic-type distribution

$$p(r)=p_0\ln\left(\frac{a(\psi)}{r}+\sqrt{\frac{a(\psi)^2}{r^2}-1}\right),\ 0<r\leqslant a(\psi),\ 0\leqslant\psi\leqslant\Psi, \tag{41}$$

where $p_0=P/(\pi a^2)$ is the mean contact pressure, $a(\psi)$ is the contact perimeter radius given by the equation

$$a(\psi)=\frac{b}{\sqrt{\lambda^2\cos^2\psi-1}}, \tag{42}$$

where λ is the eccentricity of the contact perimeter.

The contact force P, the indenter displacement w, and the characteristic size of the contact area b are connected through the system

$$w+\frac{a_0}{h}\vartheta P=\frac{\pi b}{2\tan\Theta}\frac{I_4}{I_2}, \tag{43}$$

$$\vartheta P=\frac{b^2}{2\tan\Theta}\frac{I_4}{I_1}. \tag{44}$$

The eccentricity of the contact perimeter λ and the elliptic integrals I_1, I_2, and I_4 depend on the (known) angle Ψ (see Table 1).

Again, the application of the asymptotic method for excluding the geometrical parameter of the contact area b form the system (43) and (44) yields the load-displacement relationship

$$P=\frac{I_0}{\vartheta}w^2\left(1+\frac{2I_0a_0}{h}w+\left(\frac{I_0a_0^2}{h}\right)^2w^2\right), \tag{45}$$

where we used the notation

$$I_0=\frac{2}{\pi^2}\frac{I_2^2\tan\Theta}{I_1I_4}.$$

Finally, note that by analogy with Eq. (32), the variable characteristic size of the contact zone b can be expressed in terms of the indenter's displacement w.

9. Comparisons with analytical and numerical solutions for an isotropic layer

9.1. Spherical indentation of an isotropic elastic layer

In the case of an isotropic elastic layer, we have $\gamma_1=\gamma_2=1$ and

$$\vartheta=\frac{1-\nu^2}{\pi E}, \tag{46}$$

where E is the elastic modulus, and ν is Poisson's ratio.

For an elastic layer which is bonded to a rigid base, formula (9) reduces to

$$\mathcal{L}(\lambda)=\frac{2\varkappa\sinh2\lambda-4\lambda}{2\varkappa\cosh2\lambda+1+\varkappa^2+4\lambda^2}, \tag{47}$$

where $\varkappa=3-4\nu$ is Kolosov's constant.

In the case of an elastic layer resting on a smooth rigid base, formula (12) simplifies as follows:

$$\mathcal{L}(\lambda)=\frac{\cosh2\lambda-1}{2\sinh2\lambda+2\lambda}. \tag{48}$$

Let us compare the obtained asymptotic formulas (23) and (25) with an approximate formula obtained by Dimitriadis et al. (2002), which can be written in our notation as

$$P=\frac{4h^3\alpha^3}{3\pi\vartheta R}\left\{1-\frac{2\alpha_0}{\pi}\alpha+\frac{4\alpha_0^2}{\pi^2}\alpha^2-\frac{8}{\pi^3}\left\{\alpha_0^3+\frac{4\pi^2}{15}\beta_0\right\}\alpha^3+\frac{16\alpha_0}{\pi^4}\left\{\alpha_0^3+\frac{3\pi^2}{5}\beta_0\right\}\alpha^4\right\}. \tag{49}$$

When the elastic layer is bonded to the rigid base, the dimensionless parameters α_0 and β_0 are given by

$$\alpha_0=-\frac{1.2876-1.4678\nu+1.3442\nu^2}{1-\nu},\qquad \beta_0=\frac{0.6387-1.0277\nu+1.5164\nu^2}{1-\nu}, \tag{50}$$

and, when the elastic layer is not bonded to the rigid base, they are given by

$$\alpha_0=-0.347\frac{3-2\nu}{1-\nu},\quad \beta_0=0.056\frac{5-2\nu}{1-\nu}. \tag{51}$$

First of all, observe that in both formulas (23) and (49), the factor outside the brackets has the Hertzian form, and it is readily seen that their overall structure is similar. However, we would like to emphasize that formula (49) is not asymptotically exact as $\alpha\to0$. This circumstance comes from the fact that the approximation for the contact pressure obtained in Dimitriadis et al. (2002) does not vanish at the contour of the contact area, while the contact radius itself has been determined by the Hertzian equation $a=\sqrt{wR}$. At the same time, in the fourth-order asymptotic model, the contact radius a is determined by Eq. (22). A second source of small error arises from the application of the images method for constructing Green's function entering the governing integral Eq. (4). In fact, as it is clearly seen from Eq. (48), the terms inside the brackets in (23) and (49), giving the corrections due to the finite thickness of the layer sample, should not depend on the Poisson's ratio ν, whereas according to (51), the correction terms in (49) depend on ν. Nevertheless, it should be recognized that formula (49) provides a good approximation even up to the relative radius values $a/h\approx1$ (see Figs. 1–5).

From the comparison of formulas (23) and (49), is follows that $a_0\approx-\alpha_0$ and $a_1\approx-\beta_0$, where a_0 and a_1 are determined by Eq. (14), while α_0 and β_0 are given by (50). The numerical calculations show that the error of the approximation $a_0\approx-\alpha_0$ is less than 2% for $0.15\leqslant\nu\leqslant0.5$. At the same time, the second approximation is less accurate (6% for $0.3\leqslant\nu\leqslant0.5$) and its accuracy decreases dramatically with decreasing Poisson's ratio ν.

To determine the ranges of validity of Eqs. (23), (25), and (49), we make comparisons with the numerical solution presented by Hayes et al. (1972). Note that another numerical solution was given by Sakamoto et al. (1996), and it was reported that both methods show a good agreement (maximum error is about 2%).

Table 1
Summary of the results of Giannakopoulos (2006) for the pyramidal indenters and the auxiliary parameter I_0.

Parameter	Ψ	Θ	λ	I_1	I_2	I_4	I_0
Vickers indenter	45°	68°	2.1	0.5017	0.3283	0.1889	0.5705
Berkovich indenter	60°	65.3°	2.7	0.5687	0.3386	0.1518	0.585

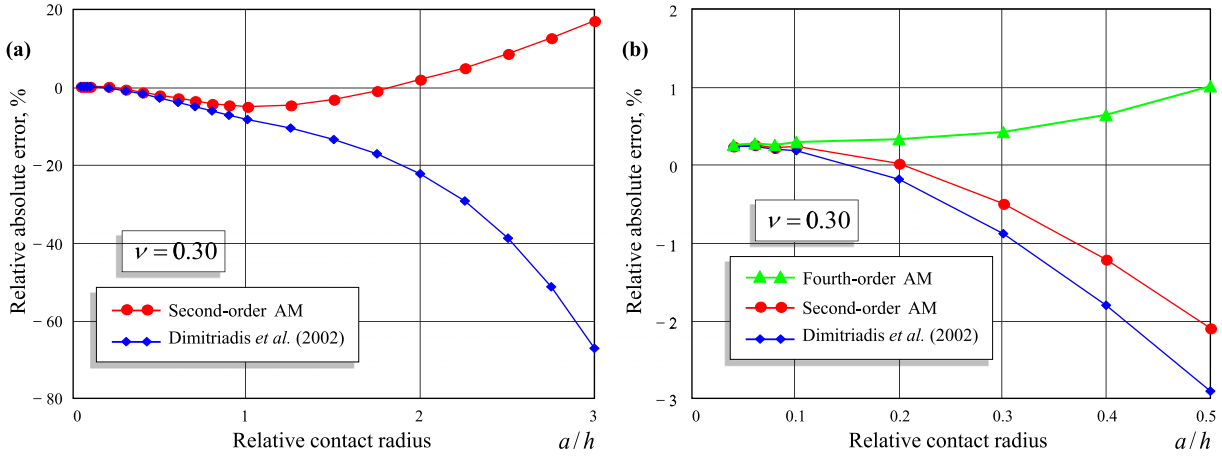

Fig. 1. Error of the analytical approximations for $\nu = 0.3$. Spherical indentation of an isotropic layer.

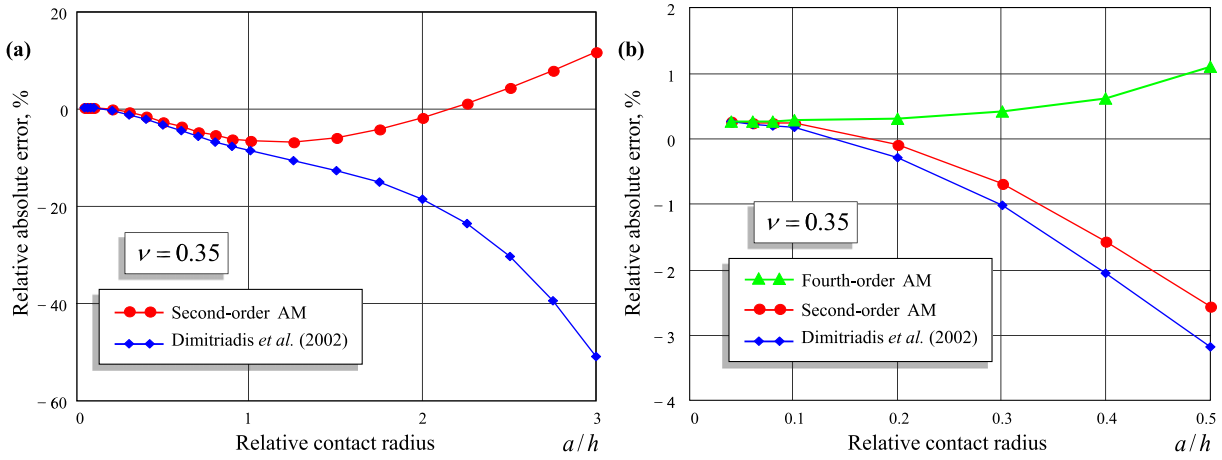

Fig. 2. Error of the analytical approximations for $\nu = 0.35$. Spherical indentation of an isotropic layer.

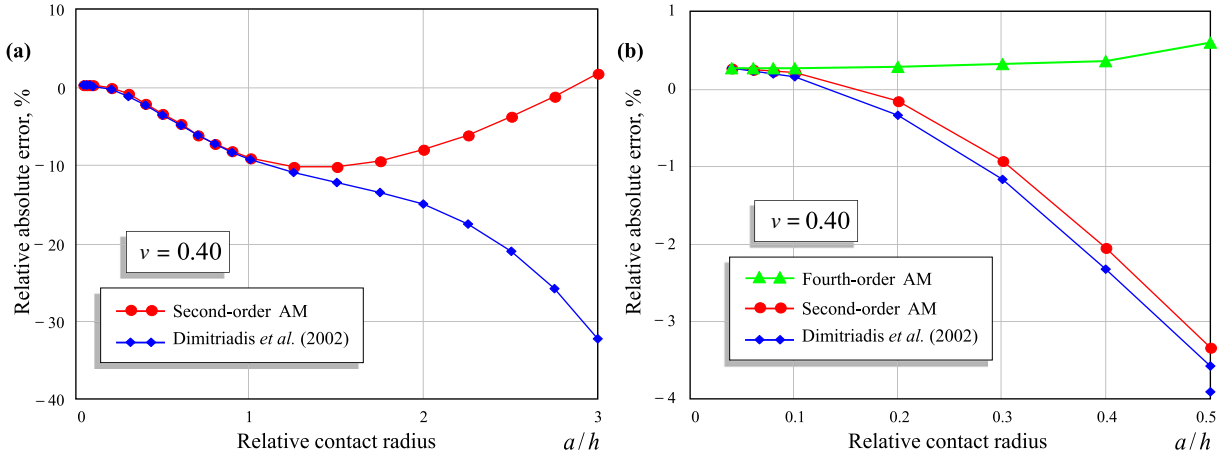

Fig. 3. Error of the analytical approximations for $\nu = 0.4$. Spherical indentation of an isotropic layer.

Comparing the second-order asymptotic formula (25) with the approximate formula (49) by Dimitriadis et al. (2002) (see Figs. 1a–5a), it should be taken into account that the last formula is of the same complexity as the four-order asymptotic formula (23). It is interesting to observe that the accuracy of the approximate formula (49) increases as Poisson's ratio approaches 0.5, whereas the accuracy of the second-order asymptotic formula (25) loses quickly its range of applicability at for incompressible materials.

Note that inside their range of validity (for small values of the dimensional parameter $\varepsilon = a/h$), the accuracy of the asymptotic models should decrease with increasing values of the parameter ε (see Figs. 1a–5a). Moreover, for those values of the parameter ε

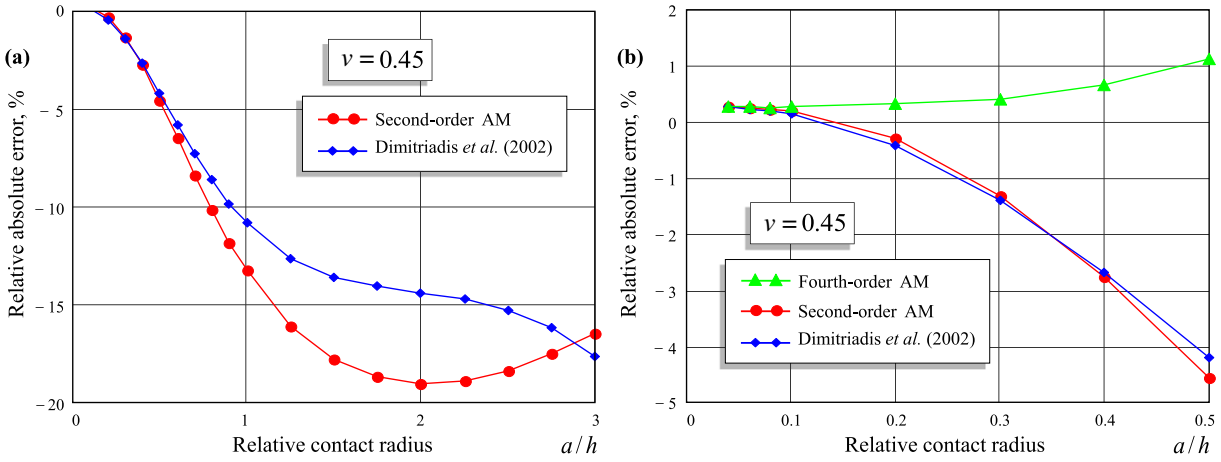

Fig. 4. Error of the analytical approximations for $\nu = 0.45$. Spherical indentation of an isotropic layer.

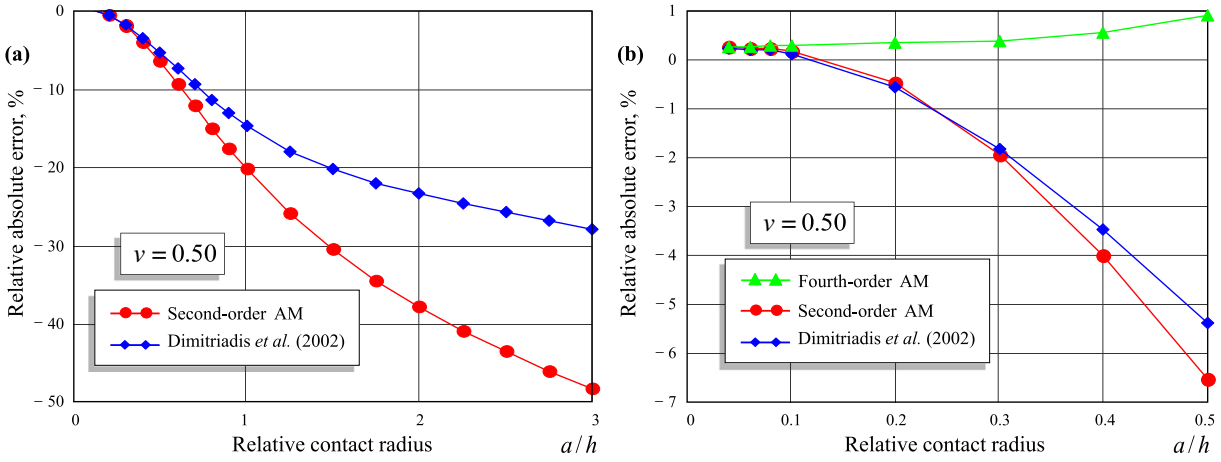

Fig. 5. Error of the analytical approximations for $\nu = 0.5$. Spherical indentation of an isotropic layer.

that cannot be considered small, asymptotic formulas, generally, do not work at all. It was observed by Dimitriadis et al. (2002) that the analytical approximation (49) has a moderate error in the range of the relative contact radius $0 \leqslant a/h \leqslant 3$ and may be used outside of its range of validity.

Finally, it should be emphasized that the accuracy of the second-order asymptotic models for the force–displacement relationship strongly depends on the value of Poisson's ratio, namely, on whether the sample material is compressible (with Poisson's ratio not too close to 0.5) or incompressible (with Poisson's ratio nearly 0.5).

9.2. Conical indentation of an isotropic elastic layer

Let us now make a comparison of the asymptotic formula (31) with the numerical solution given by Kalaba et al. (1976) in the case of an elastic layer resting without friction on a rigid substrate. Notice that as a result of non-dimensionalising, the left-hand side of their Eq. (34) should be corrected according Eqs. (28), (29b), and (29c) by dividing by wa, where w is the indenter displacement, a is the contact radius.

In the case of an isotropic elastic layer resting on a smooth rigid base, according to Eqs. (14) and (48), we have $a_0 = 1.168$. The results of numerical calculations are presented in Fig. 6 for the case $\theta = 45°$. Observe that for a relatively small contact area or, to be more precise, when the diameter of the contact area is less than the layer thickness, the accuracy of the second-order asymptotic formula (31) is less than 2.5 %.

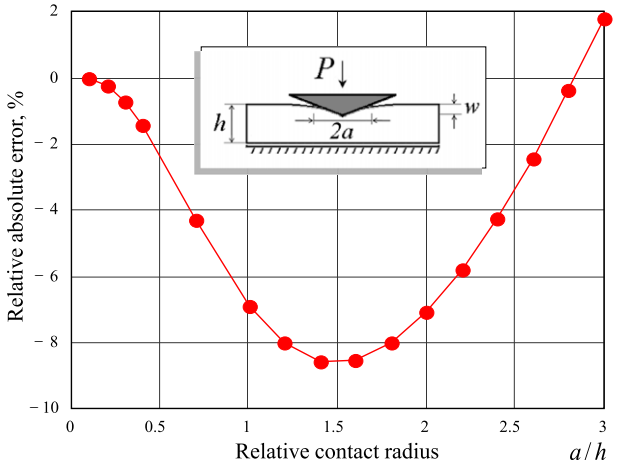

Fig. 6. Error of the second-order asymptotic model. Conical indentation of an isotropic layer.

Note that the approximations $a_0 \approx -\alpha_0$ and $a_1 \approx -\beta_0$ with Eq. (50) taken into account can be also used in the case of conical or

pyramidal indentation of an isotropic elastic layer attached to a rigid base.

10. Discussion and conclusions

Observe that the asymptotic model constructed in Section 7 can be generalized for the non-axisymmetric case when the indenter shape function satisfies the condition of self-similarity

$$\Phi(\Lambda x_1, \Lambda x_2) = \Lambda^d \Phi(x_1, x_2) \tag{52}$$

for an arbitrary positive scaling parameter Λ. Here, d is the degree of the homogeneous function $\Phi(x_1,x_2)$. In this case, according to Borodich et al. (2003), the load-displacement relationship for self-similar indentation of an elastic half-space takes the form

$$w = w_1 \left(\frac{P}{P_1}\right)^{d/(d+1)}, \tag{53}$$

where P_1 is some initial value of the external load, w_1 is the depth of indentation at this load, d is the exponent in Eq. (52).

In view of (53), the second-order asymptotic model for indentation of an elastic layer with a self-similar indenter (52) can be formulated as follows:

$$w + \frac{a_0}{h}\vartheta P = \left(w_1 + \frac{a_0}{h}\vartheta P_1\right)\left(\frac{P}{P_1}\right)^{d/(d+1)}. \tag{54}$$

By analogy with (38), we obtain

$$P = \frac{P_1}{\mathcal{W}_1} w^{\frac{d+1}{d}} \left(1 + \frac{(d+1)}{d}\frac{a_0}{h}\frac{\vartheta P_1}{\mathcal{W}_1} w^{1/d} + \frac{(d+1)(2d+3)}{2d^2}\left(\frac{a_0}{h}\frac{\vartheta P_1}{\mathcal{W}_1}\right)^2 w^{2/d}\right), \tag{55}$$

where we introduced the notation

$$\mathcal{W}_1 = \left(w_1 + \frac{a_0}{h}\vartheta P_1\right)^{\frac{d+1}{d}}.$$

Note also that Eq. (55) is valid not only in the case of frictionless contact but also for frictional contact problems (Borodich and Keer, 2004).

The present asymptotic modeling analysis is confined to the case of frictionless indentation. It is known that at micro/nano scales effects of friction and adhesion can be very important. The method for determination of mechanical characteristics of solids using JKR and DMT theories of adhesive contact (Derjaguin et al., 1975; Johnson et al., 1971) was proposed by Borodich and Galanov (2008). The second-order asymptotic model for adhesive (no-slip) spherical indentation was developed in Argatov (2010). Very recently, Espinasse et al. (2010) extended JKR and DMT contact theories for transversely isotropic materials.

The developed asymptotic modeling approach applied to the frictionless depth-sensing indentation testing has resulted in approximate (but asymptotically exact in the small-contact limit) force–displacement relationships under the assumption that the material response to indentation is described by the elastic transversely isotropic model. The second-order asymptotic models for spherical (25), conical (31), and pyramidal (45) indenters as well as for axisymmetric indenters of power-low profile (38) and self-similar non-axisymmetric indenters (55) constitute the main result of the present paper. The obtained second-order asymptotic models for the force–displacement relationship can be used for estimating the finite sample thickness effect appearing in the indentation testing of a thin sample an a rigid substrate. The applicability of the asymptotic models is governed by the ratio of the diameter of the contact area to the specimen thickness as well as by the measure of incompressibility of the sample material.

Acknowledgments

The financial support from the European Union Seventh Framework Programme under contract number PIIF-GA-2009-253055 is gratefully acknowledged. The author also would like to express his gratitude to the Referees for their helpful comments and discussions.

References

Aleksandrov, V.M., 1969. Asymptotic solution of the contact problem for a thin elastic layer. J. Appl. Math. Mech. 33, 49–63.
Aleksandrov, V.M., 2003. Asymptotic solution of the axisymmetric contact problem for an elastic layer of incompressible material. J. Appl. Math. Mech. 67, 589–593.
Alexandrov, V.M., Pozharskii, D.A., 2001. Three-Dimensional Contact Problems. Kluwer, Dordrecht.
Antunes, J.M., Menezes, L.F., Fernandes, J.V., 2006. Three-dimensional numerical simulation of Vickers indentation tests. Int. J. Solid. Struct. 43, 784–806.
Argatov, I.I., 1999. The indentation of a punch in the form of an elliptic paraboloid into the plane boundary of an elastic body. J. Appl. Math. Mech. 63, 641–649.
Argatov, I.I., 2001. The pressure of a punch in the form of an elliptic paraboloid on an elastic layer of finite thickness. J. Appl. Math. Mech. 65, 495–508.
Argatov, I.I., 2005. Asymptotic Models of Elastic Contact. Nauka, St Petersburg [in Russian].
Argatov, I.I., 2010. Frictionless and adhesive nanoindentation: Asymptotic modeling of size effects. Mech. Mater. 42, 807–815.
Barber, J.R., 1990. Contact problems for the thin elastic layer. Int. J. Mech. Sci. 32, 129–132.
Batra, R.C., Jiang, W., 2008. Analytical solution of the contact problem of a rigid indenter and an anisotropic linear elastic layer. Int. J. Solid. Struct. 45, 5814–5830.
Borodich, F.M., Galanov, B.A., 2008. Non-direct estimations of adhesive and elastic properties of materials by depth-sensing indentation. Proc. Roy. Soc. A 464, 2759–2776.
Borodich, F.M., Keer, L.M., 2004. Contact problems and depth-sensing nanoindentation for frictionless and frictional boundary conditions. Int. J. Solid. Struct. 41, 2479–2499.
Borodich, F.M., Keer, L.M., Korach, Ch.S., 2003. Analytical study of fundamental nanoindentation test relations for indenters of non-ideal shapes. Nanotechnology 14, 803–808.
Chadwick, R.S., 2002. Axisymmetric indentation of a thin incompressible elastic layer. SIAM J. Appl. Math. 62, 1520–1530.
Chen, W.T., 1971. Computation of stresses and displacements in a layered elastic medium. Int. J. Eng. Sci. 9, 775–800.
Chen, W.T., Engel, P.A., 1972. Impact and contact stress analysis in multilayer media. Int. J. Solid. Struct. 8, 1257–1281.
Cortes, D.H., Garcia, J.J., 2005. Analytic solution for the indentation of a transversely isotropic elastic layer bonded to a rigid foundation. Lat. Am. Appl. Res. 35, 167–173.
De Bruijn, N.G., 1958. Asymptotic Methods in Analysis. Noth-Holland Publ., Amsterdam.
Doerner, M.F., Nix, W.D., 1986. A method for interpreting the data from depth-sensing indentation instruments. J. Mater. Res. 1, 601–609.
Derjaguin, B.V., Muller, V.M., Toporov, Y.P., 1975. Effect of contact deformations on adhesion of particles. J. Colloid. Interface Sci. 53, 314–326.
Dimitriadis, E.K., Horkay, F., Maresca, J., Kachar, B., Chadwick, R.S., 2002. Determination of elastic moduli of thin layers of soft material using the atomic force microscope. Biophys. J. 82, 2798–2810.
Duvaut, G., Lions, J.-L., 1972. Les inéquations en mécanique et en physique. Dunod, Paris.
Elliott, H.A., 1948. Three-dimensional stress distributions in hexagonal aeolotropic crystals. Math. Proc. Cambridge Phil. Soc. 44, 522–533.
England, A.H., 1962. A punch problem for a transversely isotropic layer. Math. Proc. Cambridge Phil. Soc. 58, 539–547.
Espinasse, L., Keer, L., Borodich, F., Yua, H., Wang, Q.J., 2010. A note on JKR and DMT theories of contact on a transversely isotropic half-space. Mech. Mater. 42, 477–480.
Fabrikant, V.I., 2006. Elementary solution of contact problems for a transversely isotropic elastic layer bonded to a rigid foundation. Z. Angew. Math. Phys. 57, 464–490.
Fabrikant, V.I., 2011. Application of generalized images method to contact problems for a transversely isotropic elastic layer on a smooth half-space. Arch. Appl. Mech. 81, 957–974.
Fischer-Cripps, A.C., 2004. Nanoindentation. Springer-Verlag, New York.
Galin, L.A., 2008. Contact Problems: The Legacy of L.A. Galin. Ed. G.M.L. Gladwell, Dordrecht, Springer.
Gao, H., Chiu, C.-H., Lee, J., 1992. Elastic contact versus indentation modeling of multi-layered materials. Int. J. Solid. Struct. 29, 2471–2492.
Garcia, J., Altiero, N., Haut, R., 1998. Approach for the stress analysis of transversely isotropic biphasic cartilage under impact load. ASME J. Biomech. Eng. 120, 608–613.
Giannakopoulos, A.E., 2006. Elastic and viscoelastic indentation of flat surfaces by pyramid indentors. J. Mech. Phys. Solid. 54, 1305–1332.

Hayes, W.C., Keer, L.M., Herrmann, G., Mockros, L.F., 1972. A mathematical analysis for indentation tests of articular cartilage. J. Biomech. 5, 541–551.
Hlaváček, M., 2008. Elliptical contact on elastic incompressible coatings. Eng. Mech. 15, 249–261.
Jaffar, M.J., 1989. Asymptotic behaviour of thin elastic layers bonded and unbonded to a rigid foundation. Int. J. Mech. Sci. 31, 229–235.
Johnson, K.L., 1985. Contact Mechanics. Cambridge Univ. Press, Cambridge, UK.
Johnson, K.L., Kendall, K., Roberts, A.D., 1971. Surface energy and the contact of elastic solids. Proc. Roy. Soc. A 324, 301–313.
Jurvelin, J., Kiviranta, I., Arokoski, J., Tammi, M., Helminen, H.J., 1987. Indentation study of the biomechanical properties of articular cartilage in the canine knee. Eng. Med. 17, 15–22.
Kalaba, R.E., Yakush, A., Zagustin, E.A., 1976. On a conical punch pressing into an elastic layer. J. Elastic. 6, 441–449.
Keer, L.M., 1964. The contact stress problem for an elastic sphere indenting an elastic layer. J. Appl. Mech. 31, 143–145.
Klindukhov, V.V., 2009. Indentation of a smooth axisymmetric punch into a transversely isotropic layer. Mech. Solid. 44, 737–743.
Korhonen, R.K., Wong, M., Arokoski, J., Lindgren, R., Helminen, H.J., Hunziker, E.B., Jurvelin, J.S., 2002. Importance of the superficial tissue layer for the indentation stiffness of articular cartilage. Med. Eng. Phys. 24, 99–108.
Korhonen, R.K., Saarakkala, S., Töyräs, J., Laasanen, M.S., Kiviranta, I., Jurvelin, J.S., 2003. Experimental and numerical validation for the novel configuration of an arthroscopic indentation instrument. Phys. Med. Biol. 48, 1565–1576.
Lebedev, N.N., Ufliand, Ia.S., 1958. Axisymmetric contact problem for an elastic layer. J. Appl. Math. Mech. 22, 442–450.
Li, J., Chou, T.W., 1997. Elastic field of a thin-film/substrate system under an axisymmetric loading. Int. J. Solid. Struct. 34, 4463–4478.
Li, L.P., Cheung, J.T.M., Herzog, W., 2009. Three-dimensional fibril-reinforced finite element model of articular cartilage. Med. Biol. Eng. Comput. 47, 607–615.
Liao, J.J., Wang, C.D., 1998. Elastic solutions for a transversely isotropic half-space subjected to a point load. Int. J. Numer. Anal. Meth. Geomech. 22, 425–447.
Love, A.E.H., 1939. Boussinesqs problem for a rigid cone. Quart. J. Math. 10, 161–175.
Matthewson, M.J., 1981. Axi-symmetric contact on thin compliant coatings. J. Mech. Phys. Solid. 29, 89–113.
Sakamoto, M., Li, G., Hara, T., Chao, E.Y.S., 1996. A new method for theoretical analysis of static indentation test. J. Biomech. 29, 679–685.
Sneddon, I.N., 1995. Fourier Transforms. Dover, New York.
Stevanovic, M., Yovanovich, M.M., Culham, J.R., 2001. Modeling contact between rigid sphere and elastic layer bonded to rigid substrate. IEEE Components Packag. Technol. 24, 207–212.
Stolz, M., Gottardi, R., Raiteri, R., Miot, S., Martin, I., Imer, R., Staufer, U., Raducanu, A., Düggelin, M., Baschong, W., Daniels, A.U., Friederich, N.F., Aszodi, A., Aebi, U., 2009. Early detection of aging cartilage and osteoarthritis in mice and patient samples using atomic force microscopy. Nature Nanotechol. 4, 186–192.
Vorovich, I.I., Aleksandrov, V.M., Babeshko, V.A. 1974. Non-classical Mixed Problems of the Theory of Elasticity. Nauka, Moscow [in Russian].
Vorovich, I.I., Ustinov, Iu.A., 1959. Pressure of a die on an elastic layer of finite thickness. J. Appl. Math. Mech. 23, 637–650.
Wilson, W., van Donkelaar, C.C., van Rietbergen, R., Huiskes, R., 2005. The role of computational models in the search for the mechanical behavior and damage mechanisms of articular cartilage. Med. Eng. Phys. 27, 810–826.
Wu, J.Z., Herzog, W., 2002. Elastic anisotropy of articular cartilage is associated with the microstructures of collagen fibers and chondrocytes. J. Biomech. 35, 931–942.
Xu, H., Pharr, G.M., 2006. An improved relation for the effective elastic compliance of a film/substrate system during indentation by a flat cylindrical punch. Scripta Material. 55, 315–318.